International Journal of Quantum Information
Vol. 9, Suppl. (2011) 83–92

DOI: 10.1142/S0219749911007095

World Scientific
www.worldscientific.com

ENTANGLEMENT TRANSFER IN A MULTIPARTITE CAVITY QED OPEN SYSTEM

MATTEO BINA*,‡, FEDERICO CASAGRANDE*, ALFREDO LULLI*, MARCO G. GENONI*,† and MATTEO G. A. PARIS*

*Dipartimento di Fisica, Università di Milano, via Celoria 16, 20133 Milano, Italy

†CNISM, UdR Milano Università, 20133, Milano, Italia
‡matteo.bina@unimi.it

Received 24 August 2010

We describe the dynamics of tripartite state mapping and entanglement transfer from qubit-like radiation states to two-level atoms via optical cavity modes. When the entangled radiation is carried to the cavities by single-mode fibers, optimal pure and mixed state transfer is predicted for perfect mirror transmittance, and entanglement sudden death (and birth) is demonstrated for Werner input states. The general case of multi-mode fiber coupling is also discussed. The dynamics is finally investigated under various dissipative effects.

Keywords: Multipartite entanglement; state mapping; cavity quantum electrodynamics.

1. Introduction

The quantum correlations identified by entanglement are the key resources for several protocols of quantum information (QI) processing,[1] as for example teleportation,[2] cryptography[3] and enhanced measurements.[4] As a matter of fact, optical systems have been a privileged framework for encoding and manipulating quantum information, since bipartite and multipartite entanglement may be effectively generated either in the discrete or continuous variable regime. On the other hand, the development of QI also requires localized registers, e.g. for the storage of entanglement in quantum memories. Cavity quantum electrodynamics (CQED)[5] is a relevant scenario for this kind of investigations.

The general problem of transferring entanglement from bosonic systems to localized qubits for bipartite systems was recently addressed[6] also in the presence of some dissipative effects. In the framework of CQED the Hamiltonian description of entanglement exchange from radiation to two-level atoms was theoretically investigated[7] and the effect of cavity mode decay was numerically analyzed.[8] The literature also provides examples of similar investigations in other physical systems such as

circuit QED[9] or collective spins of atomic ensembles.[10] In the case of tripartite systems the problem of entanglement transfer was investigated in CQED for unitary dynamics.[11,12] In turn, tripartite entanglement of radiation in CV systems has been widely investigated both theoretically and experimentally (see Refs. 13–18) and, recently, photon number multipartite entanglement for qubit-like radiation states was demonstrated.[19] Another scheme for quantum state engineering has been proposed[20] allowing also entanglement purification.[21]

We recently worked out a full dynamical description of entanglement transfer from three entangled bosonic modes to three localized qubits through the action of a local environment.[22] Upon exploiting current advances in the optical regime of CQED,[19,23,24] our scheme could be implemented with three entangled radiation modes, prepared in a qubit-like state, coupled by optical fibers to three separated optical cavities containing each one a trapped two-level atom. For entangled pure input states we showed the occurrence of optimal state mapping and entanglement transfer, followed by periodical mapping of quantum correlations onto the tripartite atomic and cavity mode subsystems. In the case of external radiation prepared in a mixed Werner state we suggested a way to observe the phenomenon of entanglement sudden death/birth (ESD/ESB)[25,26] for tripartite systems. Also we showed that, during the time evolution, each subsystem (atoms or cavity modes) can alternatively exhibit different kinds of entanglement, including genuine tripartite GHZ and W entanglement. The main dissipative effects were included to obtain a realistic investigation of multipartite entanglement transfer and swapping, that is of interest for quantum interfaces and memories in quantum networks.[27,28] Here we review some basic results, extending the previous analysis by considering reflectivity losses at input cavity mirrors (subsection 3.2) and, in particular, thus providing a generalization of the treatment to the case of multi-mode fiber couplings between injected and cavity modes (subsection 3.4).

2. Model of the Physical System

The general scheme we consider is composed of an entangled three-mode bosonic system (f), prepared in general in a mixed state, which interacts with three qubits (a) through their local environments (c). The system Hamiltonian in the interaction picture is:

$$\hat{\mathcal{H}}^I = \sum_{J=A,B,C} \left[\hbar g_J(\hat{c}_J \hat{\sigma}^\dagger_J + \hat{c}^\dagger_J \hat{\sigma}_J)\right] + \sum_{J,K=A,B,C} \left[\hbar \nu_{J,K}(t)(\hat{c}_J \hat{f}^\dagger_K + \hat{c}^\dagger_J \hat{f}_K)\right] \quad (1)$$

The operators $\hat{c}_J, \hat{c}^\dagger_J (\hat{f}_J, \hat{f}^\dagger_J)$ are the annihilation and creation operators for the local environment (input bosonic) modes, while $\hat{\sigma}_J, \hat{\sigma}^\dagger_J$ are the lowering and raising operators for the target qubits in each subsystem ($J = \mathrm{A}, \mathrm{B}, \mathrm{C}$). Without loss of generality we consider real coupling constants g_J for the qubit-local environment interaction, whereas $\nu_{J,K}(t)$, that couple local environment and bosonic modes, are

taken real and time dependent in order to simulate the interaction switching-off at a suitable time t_{off}.

The optical regime of CQED is a realistic framework where our scheme may be implemented, choosing a tripartite photon-number entangled field for the bosonic modes (f), guided by optical fibers, and two-level atoms as the target qubits (a). Each qubit is trapped in a one-sided optical cavity, operating as the local environment (c). We consider the optical fibers in the short-fiber limit where radiation is carried by discrete modes.[29] In the following section, we shall distinguish the cases of single-mode and multi-mode fibers that couple to the corresponding cavities.

If the system is open, it is subjected to several dissipative effects, such as cavity losses at a rate κ_c due to interaction with a reservoir at zero temperature, atomic spontaneous emission with a decay rate γ_a, and leakage of photons from the fibers at a rate κ_f. Hence the time evolution of the whole system is described by the following master equation (ME) in the Lindblad form for the density operator $\hat{\rho}(t)$:

$$\dot{\hat{\rho}} = -\frac{i}{\hbar}[\hat{\mathcal{H}}_e, \hat{\rho}] + \sum_{J=A,B,C} \left[\hat{C}_{f,J}\hat{\rho}\hat{C}^{\dagger}_{f,J} + \hat{C}_{c,J}\hat{\rho}\hat{C}^{\dagger}_{c,J} + \hat{C}_{a,J}\rho\hat{C}^{\dagger}_{a,J}\right] \tag{2}$$

where the non-Hermitian effective Hamiltonian is

$$\hat{\mathcal{H}}_e = \hat{\mathcal{H}}^I - \frac{i\hbar}{2}\sum_{J=A,B,C}\left[\hat{C}^{\dagger}_{f,J}\hat{C}_{f,J} + \hat{C}^{\dagger}_{c,J}\hat{C}_{c,J} + \hat{C}^{\dagger}_{a,J}\hat{C}_{a,J}\right] \tag{3}$$

The jump operators for the atoms are $\hat{C}_{a,J} = \sqrt{\gamma_a}\hat{\sigma}_J$, for the fibers $\hat{C}_{f,J} = \sqrt{\kappa_f}\hat{f}_J$ and for the cavity modes $\hat{C}_{c,J} = \sqrt{\kappa_c}\hat{c}_J$. The choice of an environment at zero temperature is supported by the fact that in optical cavities thermal noise is negligible. Moreover in the optical regime spontaneous emission can be effectively suppressed and single atoms can stay trapped even for several seconds.[23] From now on we consider dimensionless parameters, all scaled to the coupling constant g_A, and times $\tau = g_A t$, introducing the dimensionless switching-off time $\tau_{off} = g_A t_{off}$.

3. Entanglement Transfer and State Mapping in the Hamiltonian Regime

In this section we shall treat the unitary dynamics of the system, described in detail in a previous work,[22] taking into account some effects like the cavity mirror transmittance, ESD and ESB phenomena for some initial mixed state and the effect of multi-mode coupling between fibers and cavities.

3.1. *Qubit-like external radiation carried by single-mode fibers*

In order to better understand the problem of transferring the entanglement from the external field to the atomic and cavity modes subsystems, we firstly consider the case of radiation coupled to the cavity modes by means of single mode fibers ($\nu_{JK} = 0$ if $J \neq K$ and $\nu_{J,J} = g_A$ for all J). This can be achieved performing the "short fiber

limit"[29] which essentially allows only a single mode of the fiber to interact with the cavity. Starting from a qubit-like entangled state $\hat{\rho}_f(0)$ all subsystems (a, c, f) behave as qubits and their multipartite entanglement dynamics can be described by combining the information from tripartite negativity,[30] entanglement witnesses[31] for the two inequivalent classes GHZ and W,[32] and some criteria for separability.[33] In fact, the tripartite negativity $E^{(\alpha)}(\tau)(\alpha = a, c, f)$, defined as the geometric mean of the three bipartite negativities,[34] is an entanglement measure that provides only a sufficient condition for entanglement detection, although its positivity guarantees GHZ-distillability.

We first illustrate the case of an external field prepared in an entangled pure state $|\Psi(0)\rangle_f$, atoms initially in the lower state $|ggg\rangle_a$ and cavities in the vacuum state $|000\rangle_c$. Overall we are dealing with an interacting 9-qubit system where the input field is switched off at the time τ_{off}, for instance by rotating the fiber polarization.

In Fig. 1, we summarize the dynamics for the external field prepared in the GHZ state $|\Psi(0)\rangle_f = (|000\rangle_f + |111\rangle_f)/\sqrt{2}$. We first describe the transient regime $0 < \tau \leq \tau_{off}$, where $\tau_{off} = \pi/\sqrt{2}$ corresponds to the maximum of the probability $p_e(\tau)$: each input qubit transfers its excitation to the cavity which in turn passes it onto the atom (see Fig. 1(a)). Each cavity mode, simultaneously coupled to the external field and to the atom, exchanges energy according to a Tavis-Cummings dynamics at an effective frequency[5,35] $g_A\sqrt{2}$ and the mean photon number $N^{(c)}(\tau) \equiv \langle \hat{c}^\dagger \hat{c} \rangle(\tau)$ in each cavity completes a cycle. In Fig. 1(b) we also see that the atomic tripartite negativity is always positive and $E^{(a)}(\tau_{off}) = 1$, that is the value for the injected GHZ state. Until τ_{off} the dynamics maps the whole initial state $|\Psi(0)\rangle_f \otimes |000\rangle_c \otimes |ggg\rangle_a$ onto the pure state $|000\rangle_f \otimes |000\rangle_c \otimes |\Psi(0)\rangle_a$, where $|\Psi(0)\rangle_a$ is obtained from $|\Psi(0)\rangle_f$ by the correspondence $|0\rangle_f \to |g\rangle_a$ and $|1\rangle_f \to |e\rangle_a$. As for the cavity mode dynamics we note that (see Fig. 1(b)) the local maximum of $E^{(c)}(\tau_{off}/2)$ does not correspond to a pure state, i.e. the initial state $|\Psi(0)\rangle_f$ cannot be exactly mapped onto the cavity modes during the transient regime. Therefore we have that entanglement is only

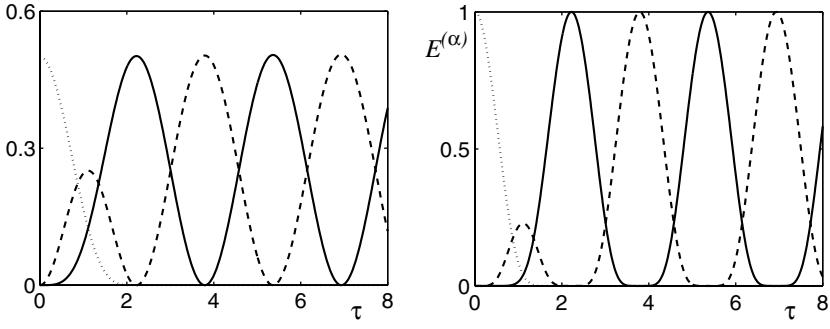

Fig. 1. Dynamics of the nine-qubit system for the external field initially prepared in a GHZ state. In (a) the average number of photons $N^{(c)}$ (dashed), $N^{(f)}$ (dotted) and the probability of excited state p_e (solid). In (b) the tripartite negativity $E^{(\alpha)}$ for atoms (solid), cavity modes (dashed) and external field (dotted).

partially transferred to the cavity modes but nevertheless this is enough for the building up of full atomic entanglement later on. At the end of the transient regime the external radiation is turned off and the subsequent dynamics is described by a triple Jaynes-Cummings[36] (JC) model ruled by oscillations at the vacuum Rabi frequency $2g_A$, hence with a dimensionless period π as shown by cavity mean photon number and atomic probability in Fig. 1(a). The analysis of the purities and the fidelities has been widely carried out in a recent work,[22] confirming the optimal state mapping. We also notice that this benchmark can be reached starting from any tripartite qubit-like pure state, which can be written in a generalized Schmidt decomposition.[32]

3.2. *Effect of cavity mirror transmittance*

By choosing to turn off the external field at times $\tau' \leq \tau_{off}$ we find a progressive degradation of the entanglement transfer to the atomic and cavity subsystems. This effect is fully equivalent to the presence of a reduced cavity mirror transmittance, which may be defined as $T(\tau') = 1 - N^{(f)}(\tau')/N^{(f)}(0)$. For several fraction of the initial mean photon number injected in the cavities (see Fig. 2(a)) we analyze the subsequent dynamics of the subsystems. In particular in Fig. 2(b) we show the time evolution of cavity mean photon number $N^{(c)}(\tau)$ and in Fig. 2(c) the atomic excitation probability $p_e(\tau)$. The influence on the entanglement transfer scheme of a reduced intensity of the transmitted radiation is well-described by the plots of the tripartite negativity for both the atomic and cavity subsystems in (Figs. 3(a) and 3(b)). As expected, the lower the input energy into the local environments, the worse is the entanglement transfer efficiency. Nevertheless even for a 10% change in the value of τ_{off}, the fidelity remains above 99.9%, i.e. entanglement transfer is robust against fluctuations of the switching-off time and this feature is a relevant one in view of possible implementations.

3.3. *Entanglement sudden death and birth*

Here we resume some results and considerations about ESD and ESB effects which occur in the time evolution of (a) and (c) subsystems starting from some peculiar

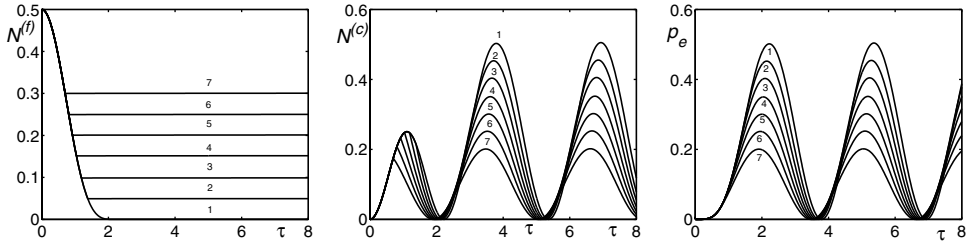

Fig. 2. Mean photon number of the external radiation and of the cavity modes and atomic excitation probability for different values of mirror transmittance: (1) $T(2.22) = 1.0$, (2) $T(1.38) = 0.9$, (3) $T(1.19) = 0.8$, (4) $T(1.04) = 0.7$, (5) $T(0.92) = 0.6$, (6) $T(0.81) = 0.5$, (7) $T(0.70) = 0.4$.

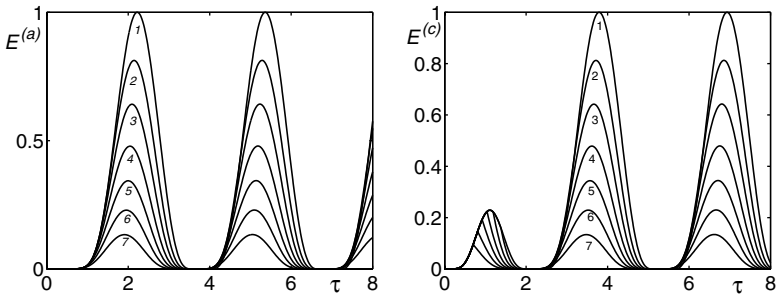

Fig. 3. Effect of cavity mirror transmittance T on the dynamics of atomic and cavity entanglement $E^{(a,c)}$: (1) $T(2.22) = 1.0$, (2) $T(1.38) = 0.9$, (3) $T(1.19) = 0.8$, (4) $T(1.04) = 0.7$, (5) $T(0.92) = 0.6$, (6) $T(0.81) = 0.5$, (7) $T(0.70) = 0.4$.

mixed states. If we consider as injected field the Werner state $\hat{\rho}_f(0) = (1-p)|GHZ\rangle\langle GHZ| + p/8\hat{I}, (0 \leq p \leq 1)$, it is possible to classify the entanglement properties for different ranges of the mixing parameters p. As soon as the evolution of the system starts, the density matrices of all subsystems lose the form of a GHZ state mixed with white noise, but still preserve invariance under all permutations of the three qubits and present only one non vanishing coherence as in $\hat{\rho}_f(0)$. Nevertheless it is still possible to single out and differentiate the genuine tripartite entanglement of GHZ and W type, from the classes of biseparable and fully separable states. In particular we find genuine tripartite ESD and ESB phenomena for the atomic subsystem and, for fixed values of p, the atomic state may exhibit transition from W to GHZ entanglement class and viceversa in a finite time. The same effects hold for the cavity modes and they are allowed by the non-unitarity of the partial trace over non-atomic degrees of freedom, which implies that the overall map on the initial three qubits is not SLOCC. We also notice that for times $\tau \geq \tau_{off}$ we can solve exactly the triple JC dynamics, thus confirming our numerical results and providing generalization of the results for mixed states.[37]

Starting, instead, from a mixed state in the form $\hat{\rho}_f(0) = p|GHZ\rangle\langle GHZ| + (1-p)|W\rangle\langle W|, (0 \leq p \leq 1)$, we cannot demonstrate ESD or ESB for these kind of states in the whole parameter space $\{p, \tau\}$, because the symmetry under qubit permutations is lost during the time evolution. We can anyway affirm that, for some fixed values of p, there is a discontinuity for the atomic full tripartite entanglement time evolution.[38]

3.4. *Entanglement transfer for multi-mode fiber coupling*

Finally, we consider multi-mode coupling of the external field to each cavity mode. For simplicity we choose equal dimensionless coupling constants $\tilde{\nu}_{J,K} \equiv \nu_{J,K}/g_A \neq 0$ if $K \neq J$ and we consider values up to 1.4. In the transient regime, the dynamics is sharply modified with respect to the case of single mode fiber shown in Fig. 1. By increasing the values of $\tilde{\nu}_{J,K}$ the period of energy exchange decreases from $2\pi/\sqrt{2}$

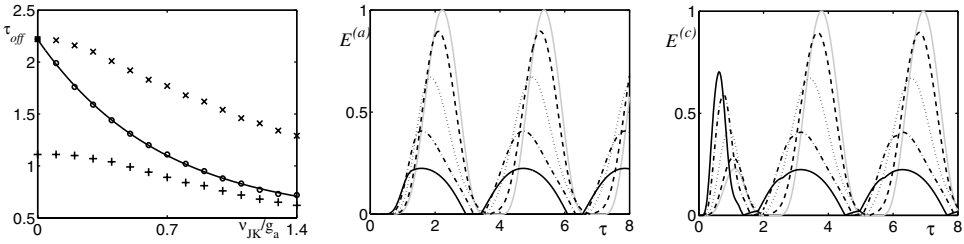

Fig. 4. Effect of multi-mode coupling. a) Dependence of $\tau_{\rm off}$ on the coupling constants $\tilde{\nu}_{J,K}$ for different choices of switching-off the external field: maximum of $p_e(\tau)$ (o), minimum of $N^{(f)}(\tau)$ (x), and maximum of $N^{(c)}(\tau)$ (+). b,c) Tripartite negativities $E^{(\alpha)}$ ($\alpha = a, c$) for $\tilde{\nu}_{J,K} = 0$ (solid gray), 0.3 (dashed), 0.6 (dotted), 1.0 (dashed-dotted), and 1.4 (solid black) when $\tau_{\rm off}$ corresponds to the maximum of $p_e(\tau)$.

to $\cong 2.6$. The maximum of cavity mode mean photon number grows up to $N^{(c)} \cong 0.41$ whereas the maximum of atomic excitation probability decreases to $p_e \cong 0.24$. The external field mean photon number does not vanish but it reaches a minimum, that can always be found between the two maxima of $N^{(c)}(\tau)$ and $p_e(\tau)$, such that $0.002 < N^{(f)} < 0.02$ changing $\tilde{\nu}_{J,K}$ from 0.1 to 1.4. We investigate the differences in the entanglement transfer for three selections of the switching-off time $\tau_{\rm off}$ corresponding to the maximum of $p_e(\tau)$, the minimum of $N^{(f)}(\tau)$ and the maximum of $N^{(c)}(\tau)$.

In Fig. 4(a) we show the dependence of τ_{off} on $\tilde{\nu}_{J,K\neq J}$. Switching off the external field at times τ_{off} corresponding to the maxima of $p_e(\tau)$, as in the previous case with single-mode fibers, we find (Figs. 4(b) and 4(c)) that the maxima of tripartite negativities $E^{(\alpha)}(\tau)$ after the transient regime reduce for increasing values of $\tilde{\nu}_{J,K}$ for both atomic and cavity mode subsystems. If we consider τ_{off} corresponding to the minimum of $N^{(f)}(\tau)$ (Figs. 5(a) and 5(b)) we observe a small reduction of the peak values of $E^{(\alpha)}(\tau)$. Finally, if we turn off the external field at the first maximum of the cavity field mean photon number we note that by increasing the values of $\tilde{\nu}_{J,K}$ it is possible to improve the entanglement transfer (Figs. 5(c) and 5(d)). The peak value of tripartite negativity grows up to $\cong 0.93$ for $\tilde{\nu}_{J,K} = 1.4$ and the fidelity up to $\cong 0.95$ for both subsystems (a) and (c). We remark that these values cannot be significantly increased for larger values of $\tilde{\nu}_{J,K}$.

In conclusion, for all the above choices of switching-off time τ_{off} we observe that, by increasing the values of $\tilde{\nu}_{J,K}$, the amount of entanglement that can be transferred to the cavity modes in the transient regime also increases. This is due to the fact that the amount of energy transferred to each cavity mode increases: in fact, the peak value of $N^{(c)}(\tau)$ progressively grows up from $\cong 0.25$ to $\cong 0.41$. Nevertheless, multi-mode coupling for larger values of τ_{off} results in a less favorite condition for entanglement transfer.

4. Dissipative Effects on the State Mapping

In the perspective of an experimental implementation of our scheme, an important issue is the detrimental effect of dissipation on both state mapping and entanglement

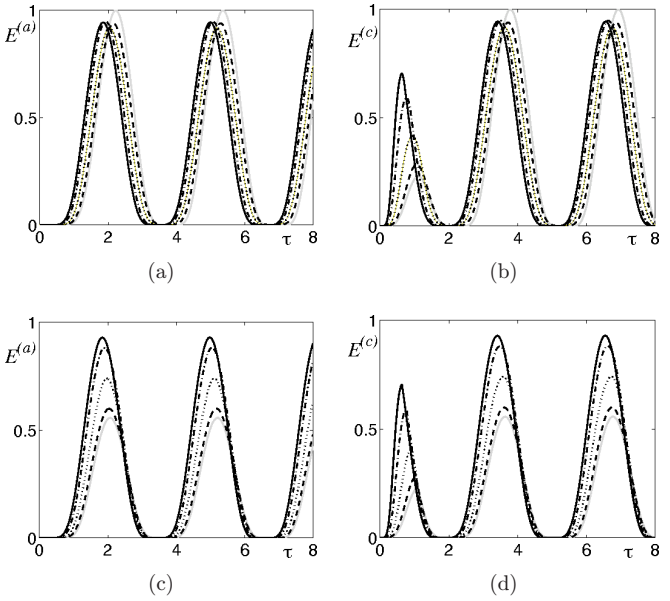

Fig. 5. Effect of multi-mode coupling on tripartite negativities $E^{(\alpha)}$ $(\alpha = a, c)$ for $\tilde{\nu}_{J,K} = 0$ (solid gray), 0.3 (dashed), 0.6 (dotted), 1.0 (dashed-dotted), and 1.4 (solid black): a,b) τ_{off} in the minimum of $N^{(f)}(\tau)$; c,d) τ_{off} in the maximum of $N^{(c)}(\tau)$.

transfer. Here we provide some examples, obtained by numerically solving the full ME (2) through Monte Carlo Wave Function method,[39] in order to give a quantitative behavior of the system in realistic conditions. Starting with an external field prepared in a GHZ pure state, we analyze the effect of cavity decay rates in the range $0 < \tilde{\kappa}_c \leq 0.5$ for negligible values of all other decay rates. We consider the fidelities $F^{(\alpha)}$ and the tripartite negativities $E^{(\alpha)}$ at the first peaks $(\alpha = c, f)$ as function of $\tilde{\kappa}_c$. In the left panel of Fig. 6 we see that all these quantities can be well-fitted by

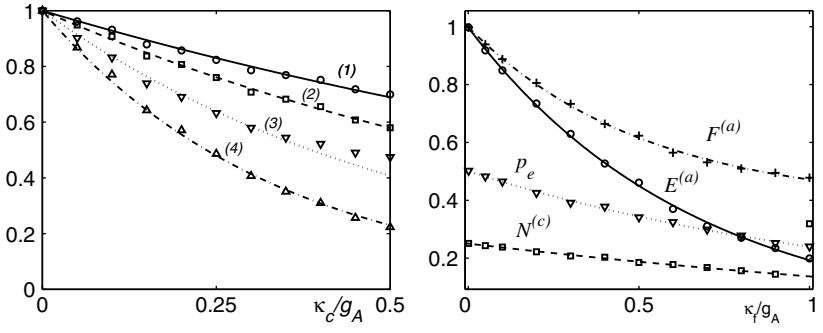

Fig. 6. (Left): Effect of cavity dissipation. Tripartite negativities at the first peak and fidelities vs. $\tilde{\kappa}_c \equiv \kappa_c/g_A$: $F^{(a)}$ (1), $E^{(a)}(2)$, $F^{(c)}$ (3), $E^{(c)}$ (4). (Right): Effect of fiber dissipation. Atomic tripartite negativity E^a(solid), fidelity F^a(dash-dot), and atomic probability p_e(dot) at time τ_{off}; cavity mean photon number $N^{(c)}$(dash) at time $\tau_{off}/2$, vs $\tilde{\kappa}_f \equiv \kappa_f/g_A$ for $\tilde{\kappa}_c \ll 1, \tilde{\gamma}_a \ll 1$.

exponential functions, with decay rates $\beta_F^{(a)} = 0.75, \beta_E^{(a)} = 1.09$ for the atomic subsystem, and $\beta_F^{(c)} = 1.80, \beta_E^{(c)} = 2.94$ for the cavity modes. As one may expect, quantum state mapping and entanglement transfer are by far more efficient onto atomic than cavity qubits. For instance, if $\tilde{\kappa}_c = 0.1$ we obtain a state mapping onto the atoms (cavity modes) with a fidelity of $\cong 0.93$ ($\cong 0.83$). Upon adding a nonzero atomic decay we see that this is a minor effect compared to cavity decay. As an example, fixing the value of atomic decay rate $\tilde{\gamma}_a = 0.03$ and cavity decay rate $\tilde{\kappa}_c = 0.1$, the fidelity of the atomic (cavity mode) subsystem reduces by 4.4% (8.9%). Finally, we address the effect of fiber losses, which is of course relevant only up to the time τ_{off}. We evaluated the effects of decay rates $\tilde{\kappa}_f$ up to 1.0 for negligible values of atomic and cavity decay rates ($\tilde{\kappa}_c \ll 1$, $\tilde{\gamma}_a \ll 1$) (see the right panel of Fig. 6). We show the effect of fiber losses $\tilde{\kappa}_f$ on cavity field mean photon number $N^{(c)}(\tau_{off}/2)$ and atomic excitation probability $p_e(\tau_{off})$ and we see that the amount of energy transferred to the atoms and to the cavity modes decreases exponentially for increasing values of $\tilde{\kappa}_f$; the decay rates are $\cong 0.42$ and $\cong 0.82$, respectively. The behavior of the tripartite negativity $E^{(a)}$ and the fidelity $F^{(a)}$ at the first peak can be described by exponential functions of $\tilde{\kappa}_f$, whose decay rates are $\cong 1.51$ and $\cong 1.95$, respectively.

5. Conclusion

We have described the mapping of quantum states and the transfer of quantum entanglement for three qubit-like radiation modes to three localized qubits via optical fibers coupled to (one-sided) optical cavities. The scheme exhibits optimal performance for input radiation prepared in GHZ or W states, and leads to tripartite ESD/ESB effects for mixed Werner states.[22] We have elucidated the dynamical description of cavity mirror reflectivity in the protocol. Moreover we have generalized the treatment in Ref. 22 to the case of multi-mode fiber coupling, showing that when the protocol is not optimal, it is possible to (partially) compensate the reflectivity losses. The open system dynamics has been also investigated to evaluate the limits dictated by cavity, atomic and fiber mode decays.

References

1. M. A. Nielsen and I. L. Chuang, *Quantum Computation and Quantum Information* (Cambridge University Press, Cambridge, 2000).
2. C. H. Bennett *et al.*, *Phys. Rev. Lett.* **70** (1993) 1895.
3. N. Gisin *et al.*, *Rev. Mod. Phys.* **74** (2002) 1458.
4. G. M. D'Ariano, P. Lo Presti and M. G. A. Paris, *Phys. Rev. Lett.* **87** (2001) 270404.
5. S. Haroche and J. M. Raimond, *Exploring the Quantum* (Oxford University Press, 2006).
6. M. Paternostro, W. Son and M. S. Kim, *Phys. Rev. Lett.* **92** (2004) 197901.
7. W. Son *et al.*, *J. Mod. Opt.* **49** (2002) 1739; M. Paternostro *et al.*, *Phys. Rev. A* **70** (2004) 022320; J. Zou *et al.*, *Phys. Rev. A* **73** (2006) 042319; F. Casagrande, A. Lulli and M. G. A.

Paris, *Phys. Rev. A* **75** (2007) 032336; A. Serafini *et al.*, *Phys. Rev. A* **73** (2006) 022312; M. Paternostro, G. Adesso and S. Campbell, *Phys. Rev. A* **80** (2009) 062318.
8. F. Casagrande, A. Lulli and M. G. A. Paris, *Eur. Phys. J. ST* **160** (2008) 71.
9. M. Paternostro *et al.*, *Phys. Rev. B* **69** (2004) 214502.
10. J. Hald *et al.*, *J. Mod. Opt.* **47** (2000) 2599; B. Julsgaard *et al.*, *Nature* **432** (2004) 482.
11. J. Lee *et al.*, *Phys. Rev. Lett.* **96** (2006) 080501.
12. F. Casagrande, A. Lulli and M. G. A. Paris, *Phys. Rev. A* **79** (2009) 022307.
13. J. Zhang *et al.*, *Phys. Rev. A* **66** (2002) 032318; J. Jing *et al.*, *Phys. Rev. Lett.* **90** (2003) 167903; T. Aoki *et al.*, *Phys. Rev. Lett.* **91** (2003) 080404.
14. M. Bondani *et al.*, *Opt. Lett.* **29** (2004) 180; A. Ferraro *et al.*, *J. Opt. Soc. Am. B* **21** (2004) 1241; A. Allevi *et al.*, *Las. Phys.* **16** (2006) 1451.
15. A. Allevi *et al.*, *Phys. Rev. A* **78** (2008) 063801.
16. A. Furusawa *et al.*, *Science* **282** (1998) 706.
17. A. S. Bradley *et al.*, *Phys. Rev. A* **72** (2005) 053805; O. Pfister *et al.*, *Phys. Rev. A* **70** (2004) 020302(R).
18. A. S. Villar *et al.*, *Phys. Rev. Lett.* **97** (2006) 140504.
19. S. B. Papp *et al.*, *Science* **324** (2009) 764.
20. A. E. B. Nielsen *et al.*, arXiv:1002.0127.
21. P. Lougovski, E. Solano and H. Walther, *Phys. Rev. A* **71** (2005) 013811.
22. M. Bina *et al.*, *Eur. Phys. Lett.* in press.
23. S. Nussmann *et al.*, *Nat. Phys.* **1** (2005) 122; K. M. Fortier *et al.*, *Phys. Rev. Lett.* **98** (2007) 233601; J. Ye, H. J. Kimble and H. Satori, *Science* **320** (2008) 1734.
24. A. B. Mundt *et al.*, *Phys. Rev. Lett.* **89** (2002) 103001; M. Keller *et al.*, *Nature* **431** (2004) 1075.
25. K. Zyczkovski *et al.*, *Phys. Rev. A* **65** (2001) 012101; C. Simon and J. Kempe, *Phys. Rev. A* **65** (2002) 052327; P. J. Dodd and J. J. Halliwell, *Phys. Rev. A* **69** (2004) 052105; T. Yu and J. H. Eberly, *Phys. Rev. Lett.* **93** (2004) 140404; C. E. López *et al.*, *Phys. Rev. Lett.* **101** (20089) 080503.
26. M. P. Almeida *et al.*, *Science* **316** (2007) 579; J. Laurat *et al.*, *Phys. Rev. Lett.* **99** (2007) 180504; A. Salles *et al.*, *Phys. Rev. A* **78** (2008) 022322.
27. J. I. Cirac *et al.*, *Phys. Rev. Lett.* **78** (1996) 3221; A. D. Boozer *et al.*, *Phys. Rev. Lett.* **98** (2007) 193601.
28. A. Serafini *et al.*, *Phys. Rev. A* **73** (2006) 022312.
29. T. Pellizzari, *Phys. Rev. Lett.* **79** (1997) 5242; S. J. van Enk *et al.*, *Phys. Rev. A* **59** (1999) 2659; A. Serafini, S. Mancini and S. Bose, *Phys. Rev. Lett.* **96** (2006) 010503.
30. C. Sabin and G. Garcia-Alcaine, *Eur. Phys. J. D* **48** (2008) 435.
31. A. Acin *et al.*, *Phys. Rev. Lett.* **87** (2001) 040401.
32. W. Dür, G. Vidal and J. I. Cirac, *Phys. Rev. A* **62** (2000) 062314.
33. O. Gühne and M. Seevinck, arXiv:0905.1349.
34. G. Vidal and R. F. Werner, *Phys. Rev. A* **65** (2002) 032314.
35. M. Tavis and F. W. Cummings, *Phys. Rev.* **188** (1969) 692.
36. E. T. Jaynes and F. W. Cummings, *Proc. IEEE* **51** (1963) 89.
37. M. Ge, L.-F. Zhu and L. Qiu, *Commun. Theor. Phys.* **49** (2008) 1443.
38. M. Bina *et al.*, *Phys. Scr. T* in press.
39. J. Dalibard, Y. Castin and K. Mølmer, *Phys. Rev. Lett.* **68** (1992) 580.